

## Supporting Information

### **Globule and Fiber Formation with Elastin-Like Polypeptides: A Balance of Coacervation and Crosslinking**

*Kirklann Lau,<sup>a</sup> Sean Reichheld,<sup>b</sup> Simon Sharpe,<sup>b\*</sup> Marta Cerruti<sup>a\*</sup>*

a) *Department of Materials Engineering, McGill University, 3610 University Street, Wong Building, 2250, Montreal, QC H3A 2B2*

b) *Molecular Medicine, Hospital for Sick Children, 686 Bay St., Toronto, ON M5G 0A4*

\*To whom correspondence should be addressed: [marta.cerruti@mcgill.ca](mailto:marta.cerruti@mcgill.ca), and [ssharpe@sickkids.ca](mailto:ssharpe@sickkids.ca)

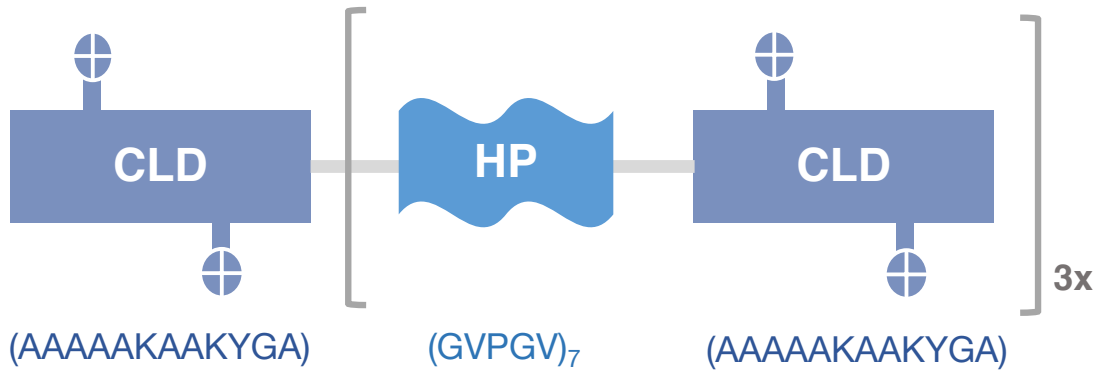


**Figure S1:** Schematic of ELP<sub>3</sub>'s repeating peptide sequence derived from both common hydrophobic (labeled HP) domain motifs and common crosslinking domain (labeled CLD) motifs found in native tropoelastin <sup>1</sup>.

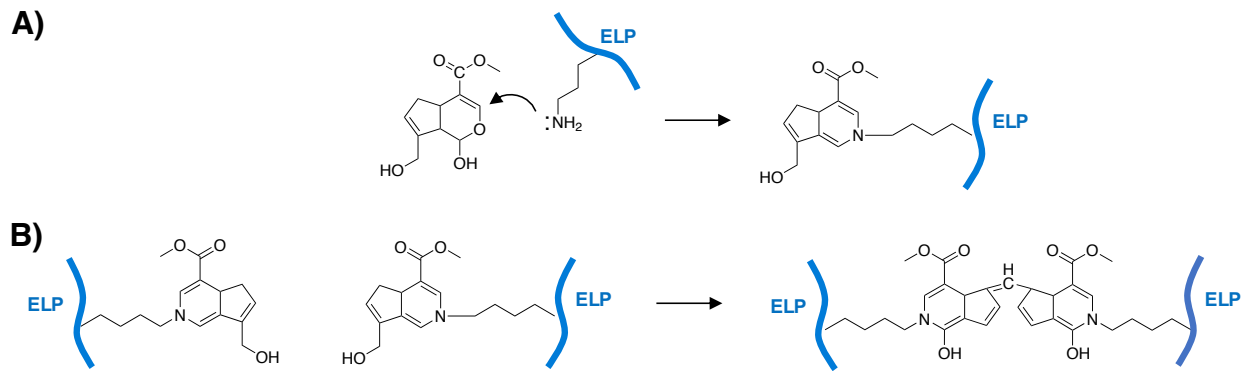


**Figure S2:** Proposed genipin crosslinking reaction pathway, which begins with A) capping reactions of free amines and ends with B) genipin dimerization into covalent crosslinks <sup>2,3,4</sup>.

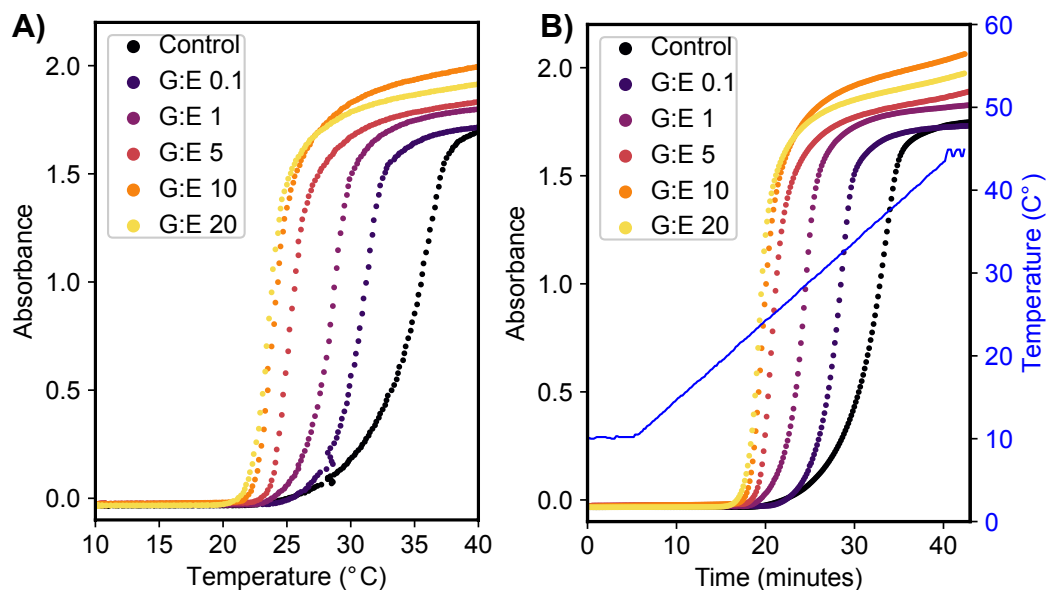


**Figure S3:** UV-vis kinetic studies of the effect of genipin concentration on ELP<sub>3</sub> coacervation, where both plots are of the same representative dataset. Absorbance on the left axes of both graphs are measured at 440nm, corresponding to the scatter plots. G:E refers to the genipin to ELP molar ratio, where the control condition has no genipin added. A) Plot of absorbance versus temperature of the reaction chamber. B) Absorbance versus time, with temperature versus time plotted on the secondary right axis. The right axis corresponds to the thin blue line plot. The plot over time highlights how the rate of coacervation also changes with genipin concentration. No stirring was used to make these measurements, since added entropy would accelerate coacervation, making it harder to observe subtle shifts in steepness of the absorbance curves over time.

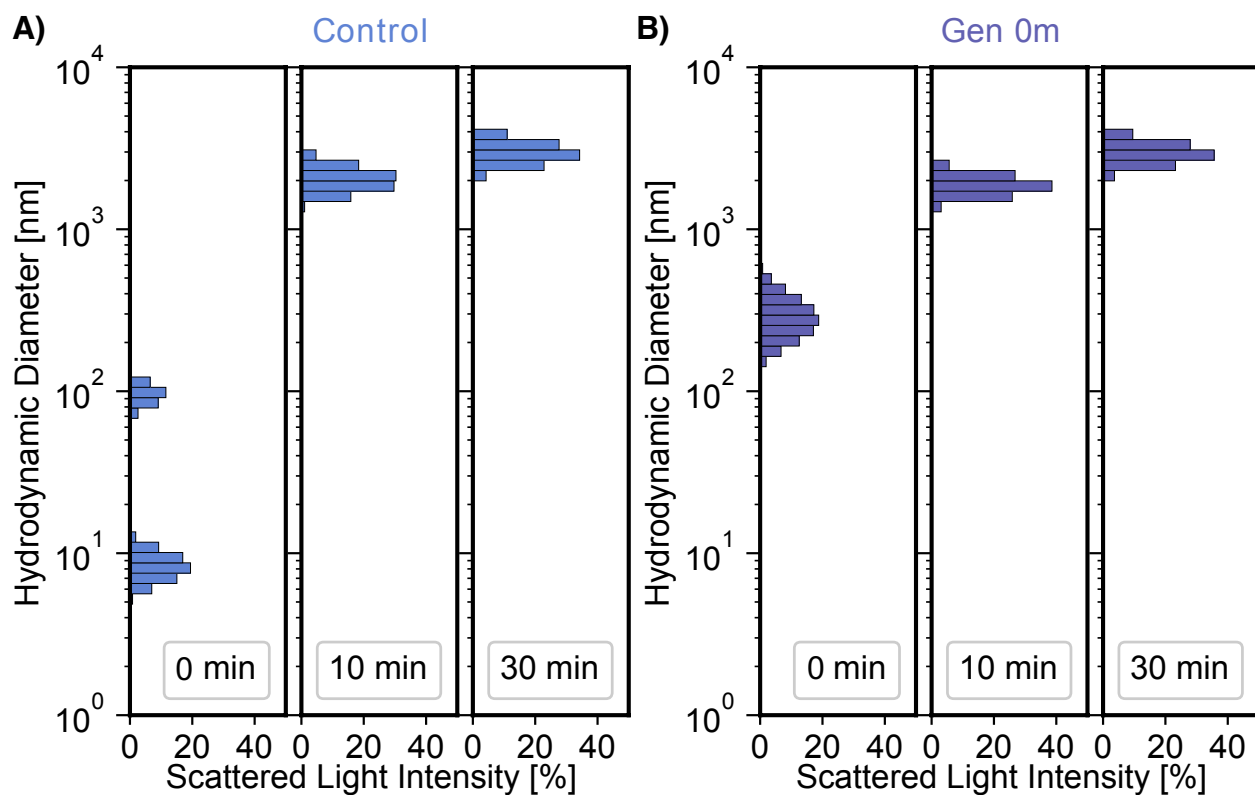


**Figure S4:** Dynamic light scattering measurements of percentage intensity size distribution of ELP<sub>3</sub> coacervate droplets in buffer solution after 0, 10, and 30 minutes from the initiation of coacervation. In practice, each measurement required a 30 second integration time, which adds error on the timepoint precision. A) Control condition where no genipin was added. B) Gen 0m condition where genipin crosslinker was added to the solution immediately before starting the experiment. Genipin was added at an ELP<sub>3</sub> molar ratio of 20:1.

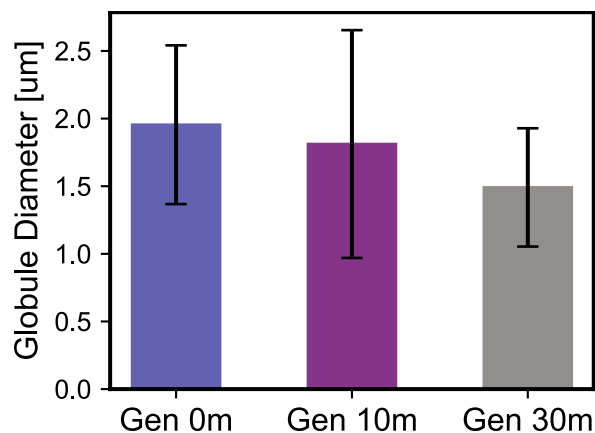


**Figure S3:** Image analysis of globule diameters visible in the SEM images seen in Figure X A), B), and C). Error bars = 1 standard deviation, where the sample size of globules counted is  $n = 150, 100, 194$  respectively.

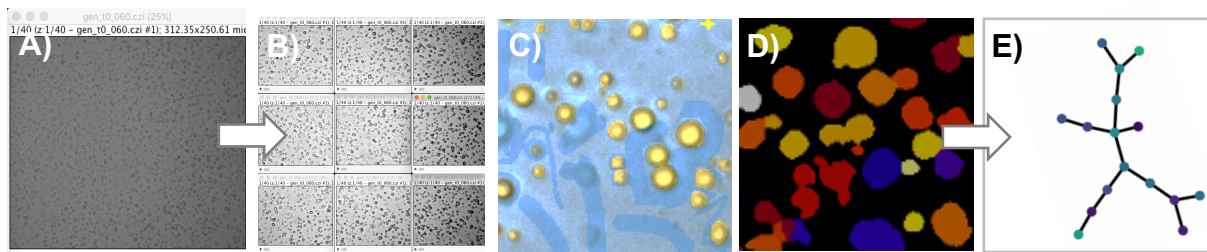


**Figure S4:** 3D image processing pipeline used to analyze droplet connectivity.

A) Raw input. 3D microscopy image stack. Each 3D image stack represents a volume of  $312 \times 250 \times 40 \mu\text{m}$ .

B) Auto-contrast and volume cropping. ImageJ was used to fix image stack contrast and crop the image stacks into smaller volume of interest with dimensions  $104 \times 83.3 \times 20 \mu\text{m}$ . This smaller volume size was analyzed to reduce computation times and to reduce background contrast variation.

C) Pixel classification. Pixels from the image stack were labeled into two categories, an  $\text{ELP}_3$  droplet phase or a solvent phase. This was performed using Ilastik, an open source software tool that uses supervised learning and a random forest classifier to segment and identify pixels.<sup>5</sup> Subregions of 3d-image stacks are manually selected by the user to train a model that labels the entirety of the respective 3d-image stack. The 3d labeling produces a probability map of the likelihood a region is either  $\text{ELP}_3$  or solvent. For supervised learning, the user corrects any mislabelling iteratively to improve the model until visually satisfactory. In our analysis, each optical 3d-image from each timepoint and condition was labeled using subregions of itself as training data. Dramatic changes in droplet shape between the different conditions prevented the training of a single broad context model for all timepoints and conditions.

D) Droplet segmentation. Once the image is separated into two different categories, individual droplets must be defined and separated so they can be counted and quantified. Following 3d labeling, Ilastik's 3d object classification tool was manually tuned for each timepoint to segment the 3d probability map into separate but connected droplets. From these segmented datasets, the ImageJ plugin MorpholibJ was used to generate 3D regional adjacency graphs, which list each unique droplet, and all the neighboring droplets that are adjacent to that droplet.<sup>6</sup> MorpholibJ also stores critical data about each droplet's voxel volume among other geometric parameters. The neighboring droplet criterion is defined to be when two voxel volumes are directly adjacent in 3d space. One limitation of this criterion is that if two non-connected droplets happen to be separated by a distance smaller than our resolution limit ( $0.23 \times 0.23 \times 1 \mu\text{m}$ ), the pair may incorrectly be counted as a connection.

E) Network analysis. Using a python script and the NetworkX python package, we visualized the regional adjacency graphs exported from the previous step. Nodes are the dots that represent droplets, and edges are the lines connecting droplets that represent physical connections. Spatial distribution of these graphs have no correlation to actual position of droplets in the images. The color of nodes seen in this example image was used to represent the volume of the original droplet. For a more detailed dataset that uses these graph visualizations, see **Figure S5**. Due to a voxel size resolution limit of  $0.23 \times 0.23 \times 1 \mu\text{m}$  from our imaging conditions, network analysis includes only populations of droplets larger than  $1 \mu\text{m}^3$ . In addition, network analysis was confined to droplets entirely within our volume of interest to avoid edge effects and inaccurate droplet volumes.

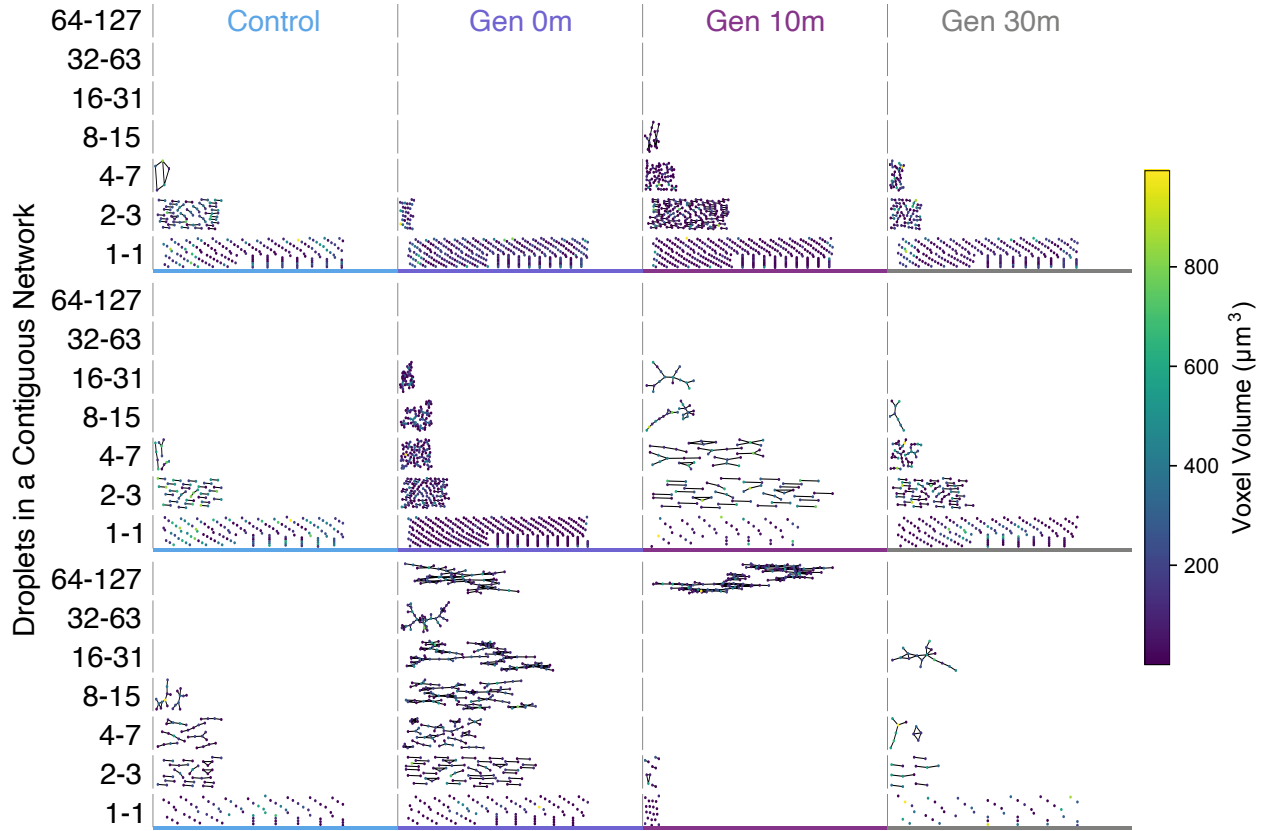


**Figure S5:** Network histograms of the effect of timing of genipin crosslinker addition on droplet size and network formation. This is an alternative visualization of the dataset seen in Figure 6. For details, see **Figure S4**. The three rows of graph represent the time evolution of the growth of droplet networks at 30m, 60m, and 90m after the inducing of coacervation. The four columns from left to right are a control condition without any genipin added, and genipin added at  $t = 0m$ , 3)  $t = 10m$ , and 4)  $t = 30m$  after inducing coacervation. Each histogram bin is sized exponentially, counting the number of droplets in a contiguous network detected.

## References

- 1 S. E. Reichheld, L. D. Muiznieks, F. W. Keeley and S. Sharpe, *Proc. Natl. Acad. Sci.*, 2017, **114**, E4408–E4415.
- 2 M. F. Butler, Y.-F. Ng and P. D. A. Pudney, *J. Polym. Sci. Part Polym. Chem.*, 2003, **41**, 3941–3953.
- 3 J. S. Yoo, Y. J. Kim, S. H. Kim and S. H. Choi, *Korean J. Thorac. Cardiovasc. Surg.*, 2011, **44**, 197–207.
- 4 C. Ninh, A. Iftikhar, M. Cramer and C. J. Bettinger, *J. Mater. Chem. B*, 2015, **3**, 4607–4615.
- 5 C. Sommer, C. Strahle, U. Köthe and F. A. Hamprecht, in *2011 IEEE International Symposium on Biomedical Imaging: From Nano to Macro*, 2011, pp. 230–233.
- 6 D. Legland, I. Arganda-Carreras and P. Andrey, *Bioinformatics*, 2016, **32**, 3532–3534.